ChemComm

Accepted Manuscript

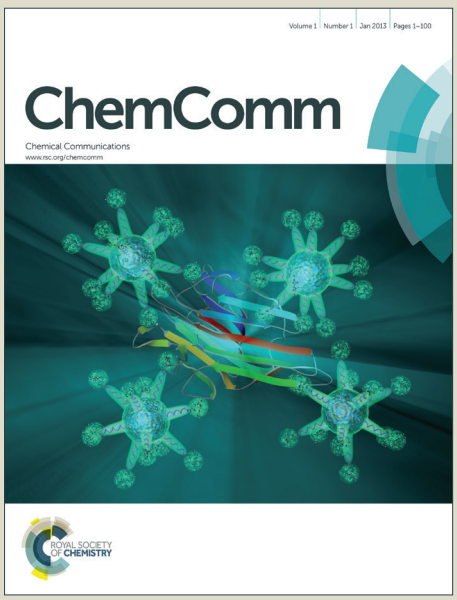

ROYAL SOCIETY OF CHEMISTRY

www.rsc.org/chemcomm

ChemComm

RSCPublishing

COMMUNICATION

Gold-plated magnetic polymers for highly specific enrichment and label-free detection of blood biomarkers under physiological conditions†

Cite this: DOI: 10.1039/x0xx00000x

Received 00th January 2014
Accepted 00th January 2014

DOI: 10.1039/x0xx00000x

www.rsc.org/chemcomm

Seung-Ryong Kwon,[a] Chang Su Jeon, [a] Nam Young Hong,[b] Kwang Pyo Kim,*[b] Inseong Hwang*[a] and Taek Dong Chung*[a]

A mass-based label-free detection of blood biomarkers in physiological conditions is realised using gold-plated magnetic polymer microspheres covered with self-assembled monolayers of polyethylene glycol alkanethiolates that effectively prevent heavy nonspecific binding of serum proteins.

A rapid, sensitive detection and quantification of biomarkers in complex physiological samples are of importance for disease diagnosis.[1] Such disease-associated macromolecules, existing in very low levels in blood, continue to be discovered and relate their *in situ* concentrations to the degree of disease progression.[2] Thus, multiplex detection of biomarkers becomes prerequisite, which would be ideally complemented by label-free sensing technologies, such as suspension arrays[3] and MALDI-TOF MS.[1c,4] While the high sensitivity and broad detection range of MALDI-TOF MS have spurred proteomics research, detection of specific biomolecules requires efficient enrichment using affinity probe-conjugated nanoparticles[4a,4b,5] or magnetic microspheres.[6] Especially, microspheres, coupled with the advances in flow cytometry technologies, have improved clinical diagnoses by allowing high throughput screening of drugs, genes, and proteins.[7] Despite their great potential, mutually exclusive obstacles such as dilution factors and matrix effects continue to limit the assay performance; an inappropriate diluent and dilution factor may lead to a clinically irrelevant result,[8] while real-life physiological matrices (blood, serum, or pleural effusion) induce heavy nonspecific binding to the solid supports.[4a,7b,9] Such unwanted biofouling inevitably masks sensor surfaces, reducing not only the specificity and sensitivity but the accuracy of quantification.[4d,10] In cases of label-free assays, nonspecific binding brings more negative repercussions because any biomolecule that binds to the sensor will produce signal.[1c] In an effort to address the issue, Davis and coworkers employed PEG-thiol self-assembled monolayers (SAMs)[11] and zwitter ionic poly-carboxybetaine methacrylate (pCBMA)[12] on Au electrodes for an electrochemical detection of a single protein biomarker in neat blood

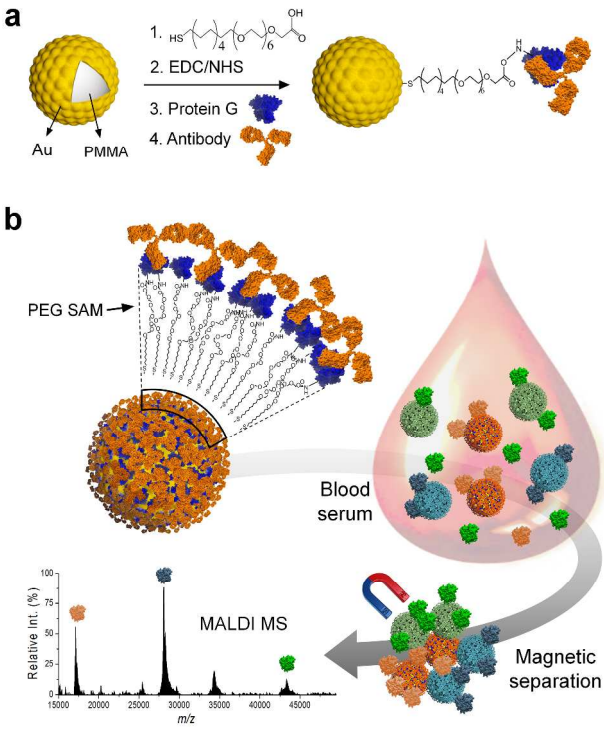

Fig. 1 Schematic illustration of manufacturing the affinity probe-conjugated magnetic gold microspheres (MGMs) (a) and their applications to the enrichment of target proteins in human serum for multiplexed label-free mass analysis (b).

[a]*Department of Chemistry, Seoul National University, Seoul 151-747, Korea, E-mail: inseong@snu.ac.kr, tdchung@snu.ac.kr.*
[b]*Department of Applied Chemistry, Kyung Hee University 1732, Deogyeong-daero, Giheung-gu, Yongin-si, Gyeonggi-do 446-701, Korea, E-mail: kimkp@khu.ac.kr*

† Electronic Supplementary Information (ESI) available. See DOI: 10.1039/b000000x/

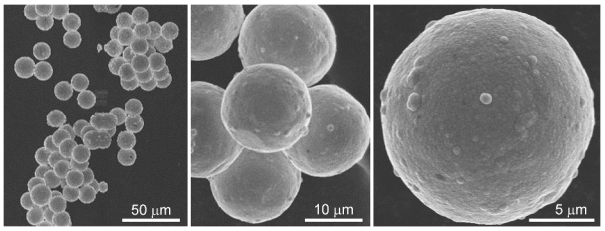

Fig. 2 FE-SEM images of MGMs 15 μm in diameter.

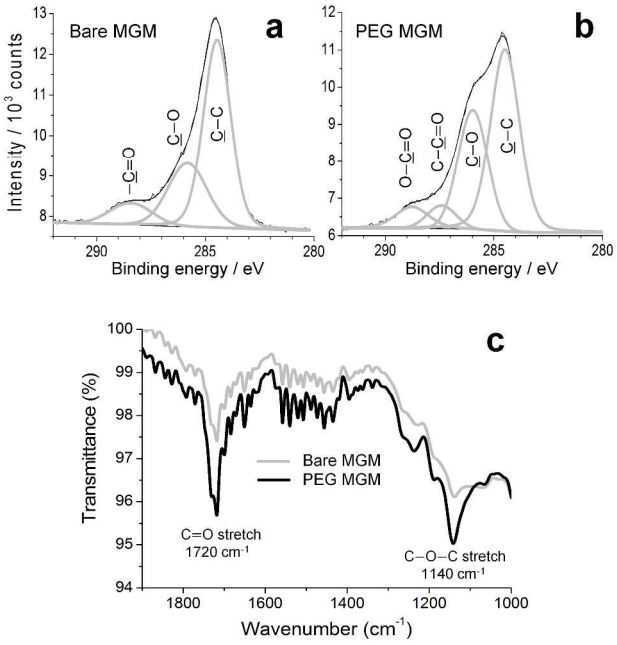

Fig. 3 C1s XPS spectra of a bare surface of MGMs (a) and the MGMs treated with carboxyl-terminated PEG-alkanethiolates (b). c) Attenuated total reflectance-Fourier transform infrared (ATR-FTIR) spectra of bare MGMs (gray line) and the MGMs treated with carboxyl-terminated PEG-alkanethiolates (solid line).

serum. The results imply that high density of hydrophilic and charged moiety is required for the efficient protection of biofouling. Previously, we showed that polymer beads, when protected with thin gold layers and PEG SAMs, exerted superior enrichment and isolation of the target molecules in intact serum, while bare polymer beads could not.[13] Herein, on the basis of previous results, we systematically compare the nonspecific binding of serum proteins and the enrichment capability between the Au-plated magnetic microspheres (MGMs) and the other microspheres, and thereby propose an extended applicability of the MGMs to a label-free detection of multiple biomarkers using MALDI-TOF MS (Fig. 1).

To investigate the degree of nonspecific bindings and target enrichment, we chose myoglobin (Myo), a 17 kDa biomarker for cardiovascular disease (CVD) as a model target. Myo exists at tens of ng mL^{-1} in normal human sera, whereas during acute myocardial infarction its population increases within three hours.[14] We compared MGMs with four types of microspheres that are broadly used for diagnostics and bioseparations: carboxyl-functionalized magnetic polymer beads (7.9 μm in diameter, Bangs Lab) carboxyl-functionalized polymer beads (15 μm in diameter, Bangs Lab), and protein G-conjugated magnetic beads with the diameter of 2 μm (New England Biolabs) and 2.8 μm (Dynabeads, Life Technologies). We initially generated SAMs on MGMs using carboxyl-terminated hexa(ethylene glycol) undecane thiol.[13] After the SAM formation, recombinant protein G was conjugated with the carboxyl group of the SAM molecule using 1-ethyl-3-(3-dimethylaminopropyl)-1-carbodiimide hydrochloride (EDC) and *N*-hydroxysuccinimide (NHS).[15] Likewise, the carboxyl-functionalized polymer microspheres were directly modified with protein G using EDC/NHS chemistry. Myo antibodies were then immobilized via protein G-Fc heavy chain interactions, rendering both antigen binding Fab chains optimally exposed to the assay media. Such oriented antibodies usually increase total antigen binding activity as compared to that of randomly oriented antibodies.[16] For MGMs, each modification step, magnetic properties, and the capability of Myo enrichment from PBS solution were verified using MALDI MS (ESI, Fig. S1-S3†).

We used ~12400 MGMs for the adsorption assays because the number of MGMs for adequate MALDI assays ranges from ~8200 (10 μg) to ~49500 (60 μg) for 0.5 mL serum samples (data not shown). The amount of antibodies immobilized on ~12400 MGMs was ~30 ng, lower than theoretical amount (ESI, Fig. S4†). For comparison, we used the same number (~12,400) of 15 μm polymer beads for the surface functionalization. The number of 7.9 μm magnetic beads was adjusted to ~44600 so that the surface area of the beads matches to the one of the MGMs. In the case of commercial protein G magnetic beads (2 and 2.8 μm), the amount of microspheres was set to capture ~30 ng of antibodies according to the manufacturers' protocols. Following SDS-PAGE analysis revealed that the commercial microspheres hold greater amount of antibody than the MGMs do except the 15 μm polymer beads (ESI, Fig. S5†). When we conducted enrichment assays using the antibody-loaded microspheres, all commercial beads, except the 15 μm polymer beads, successfully yielded Myo peaks in MALDI spectra (ESI, Fig. S6 and S7†). Importantly, nonspecific peaks corresponding to human serum albumin (HSA) always appeared in all the cases of commercial beads. In contrast, the MGMs barely yielded such nonspecific peaks except an additional peak corresponding to protein G at 23 kDa due to desorption of the SAM molecules.[17]

When we compared the relative amount of Myo enriched from the serum samples, the MGMs exhibit the highest peak intensity of Myo compared with the other commercial beads (ESI, Fig. S6f†). The MGMs show about seven-fold higher peak intensities than the 2 μm and 7.9 μm beads (~12400 beads) do despite the amount of loaded antibodies is similar to each other (ESI, Fig. S6g†). Although the Dynabeads were able to hold more than twofold antibodies (~68 ng), the relative peak intensity of Myo was fourfold lower than the one from the MGMs. When we adjusted the surface area by increasing the number of beads up to ~44600, the 7.9 μm beads could carry threefold antibodies (~95 ng), while showing about a half of the MGMs peak intensity. Therefore, we confirmed that the MGMs exceptionally enriched the target antigen in serum samples

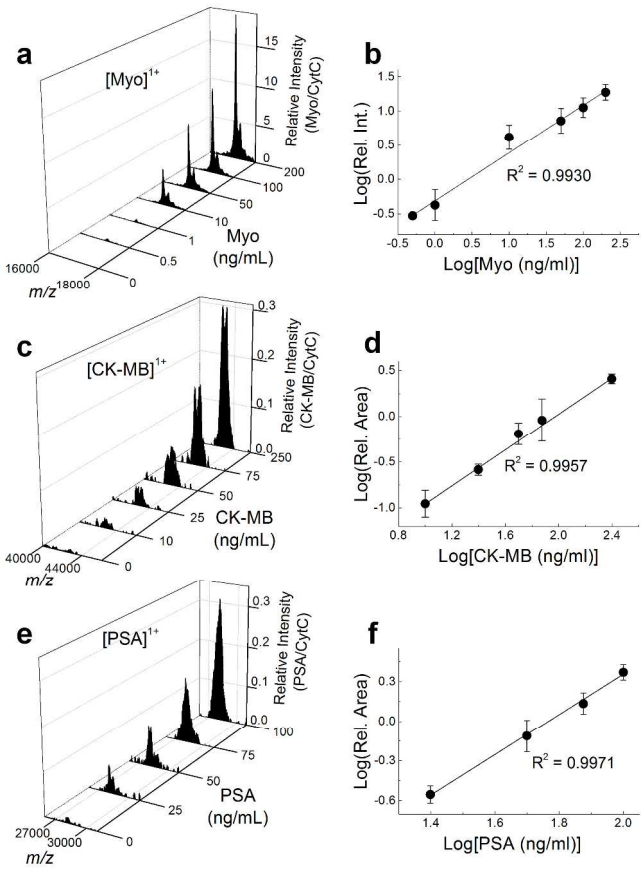

Fig. 4 Quantitative analysis of biomarkers in intact serum. Representative MALDI-TOF mass spectra with a serial dilution of Myo (a), CK-MB (c), and PSA (e) in human serum. Standard calibration curves of Myo (b), CK-MB (d), and PSA (f) are shown below. Throughout the experiments, CytC was used as an internal standard. The error bars represent the standard deviations of three independent measurements.

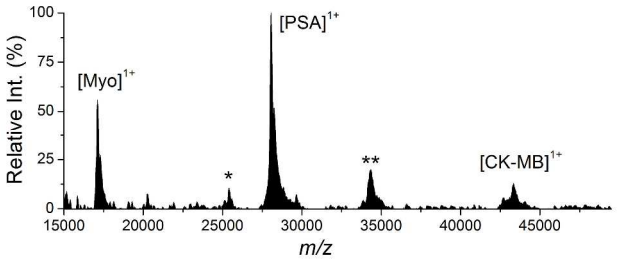

Fig. 5 MALDI-TOF mass spectrum for multiplex analysis obtained from 0.5 mL human serum spiked with 25 ng Myo, 50 ng PSA, and 50 ng CK-MB. The peaks at 26 (*) and 34 kDa (**) originate from antibodies.

even with the least amount of antibodies among the beads tested. This may be attributed to the effective isolation of the polymer core from the bulk serum proteins using SAM-Au layer; the van der Waals interaction of the aliphatic carbon chains induces a dense packing of the SAM molecules[18] and thereby provide high-density PEG groups sufficient for the suppression of nonspecific binding of serum proteins.[19]

Indeed, the density of the carboxyl groups of the PEG-alkanethiolates on MGMs was determined to be 9.2×10^{14} molecules cm^{-2} by colorimetric method (ESI, Fig. S8†),[20] about two-fold higher than the density of typical alkanethiolate SAMs on flat Au surface[21] and PEG-alkanethiolate SAMs on Au nanoparticles.[22] This extraordinary density of PEG molecules can be ascribed to the uneven nanoparticular surface structure of the MGMs that extends accessible surface area (Fig. 2). In comparison, the density of carboxyl groups of the 7.9 μm magnetic polymer beads was four-fold higher than the one of the MGMs, which is roughly in agreement with the ratio of the amount of the immobilized antibody (see Fig. S6g†). The 15 μm beads have two-fold lower carboxyl contents than the MGMs, comparable to the normal carboxyl alkanethiol SAM on flat Au surface.

The formation of PEG-alkanethiolate SAM on the MGMs was further analysed by X-ray photoelectron spectroscopy (XPS) and attenuated total reflectance-Fourier transform infrared (ATR-FTIR) spectra (Fig. 3). The C1s XPS spectrum of the bare MGMs exhibits three species of C–C, C–O, and C=O, originating from the chemical ingredients used for the synthesis of MGMs, at 284.5, 285.8, and 288.4 eV, respectively (Fig. 3a).[23] After treating the MGMs with carboxyl-terminated PEG-alkanethiolates, the peak for C–O at 284.5 eV increased and two distinct peaks for C–C=O and O–C=O appeared at 287.4 and 288.8 eV, respectively, indicating the formation of carboxyl PEG layer on the MGMs (Fig. 3b). ATR-FTIR spectra of the bare and SAM-protected MGMs also show very similar results to the XPS data; strong increases of the absorption bands near 1140 and 1720 cm^{-1}, representing the C–O stretching of the PEG groups and the C=O stretching of the carboxylic groups (Fig. 3c).

We then conducted quantification of Myo in human sera using MGMs and MALDI-TOF MS to verify the potential use of the MGMs for clinical diagnosis. Fig. 4a shows representative MALDI mass spectra obtained from the MGMs incubated with serum samples spiked with Myo ranging 0.5-200 ng mL^{-1}. As shown in Fig. 4b, the standard curve obtained from three independent experiments shows a good linear relationship ($R^2 = 0.9930$). The empirical limit of detection (LOD) is 0.5 ng mL^{-1} (0.25 ng in 0.5 mL of serum sample) with 13.4 of signal-to-noise ratio. This subnanogram LOD of the MGMs using intact serum is quite promising in that the mass spectrometry-based immunoassays using magnetic nano- or microparticles require either PBS or diluted serum as incubation media while giving no better than 1–5 ng of detection limits.[4a-c,5b]

We additionally quantified other serum biomarkers such as PSA and CK-MB to broaden the feasibility of the MGMs in protein enrichment. Unlike the Myo antibody, the antibodies for PSA and CK-MB, when immobilized onto protein G, failed to enrich the antigens probably because of less strong binding of mouse IgG1 isotype to protein G (ESI, Fig. S9†). Only when we directly conjugate the antibodies with the SAM molecules on MGMs using EDC/NHS chemistry do we observe CK-MB and PSA in human sera with 10 and 25 ng mL^{-1} of detection limit, respectively (Fig. 4c-f and

Table S1†). In contrast, without protein G mediator, we failed to enrich any of the antigens using 7.9 and 15 μm microspheres (data not shown). That the MGMs can forgo the protein G mediation itself augurs well for their approach to physiological fluid in which plenty of human serum antibodies possibly replace the protein G-bound input antibodies.

By taking advantage of innate ability of MALDI MS in simultaneous identification of multiple macromolecules, we performed multiplex detection of all three biomarkers spiked in human serum. For this experiment, we modified the MGMs with antibodies for Myo, PSA, and CK-MB without protein G. As expected, all three antigens dominantly appeared in the mass spectra without any accompanying serum proteins, consolidating the anti-fouling ability of the MGMs (Fig. 5 and Fig. S10†).

The successful integration of suspension arrays with label-free detection methods will undoubtedly ensure a forefront technology for multiplex assays. However, only a highly effective prevention of nonspecific binding would realise clinical approach of such label-free assays. The Au surface layer of the MGMs enables facile formation of PEG-SAM molecules, efficiently preventing nonspecific adsorptions owing to the dense packing of SAM molecules and thus make erroneous serum dilution obsolete. Thus, the Au-coated microspheres render label-free detection of multiple biomarkers by merging the benefits of MALDI MS and functional SAM-Au layers, paving the fundamental path for the rapid multiplexed immunoassays.

This work was supported by the Global Frontier R&D Program on Center for Multiscale Energy System (2012M3A6A7055873) funded by the National Research Foundation (NRF) and the NRF Grant (2012R1A2A1A03011289) under the Ministry of Science, ICT & Future Planning of Korea, the Basic Science Research Program funded by the NRF (2013R1A1A2006909), and the Korea Healthcare Technology R&D Project (A121987) and the National Project for Personalized Genomic Medicine (A111218-CP02) funded by the Korean Ministry for Health & Welfare.

Notes and references

1. (a) L. Hartwell, D. Mankoff, A. Paulovich, S. Ramsey and E. Swisher, *Nat. Biotechnol.*, 2006, **24**, 905-908; (b) A. Csordas, A. E. Gerdon, J. D. Adams, J. R. Qian, S. S. Oh, Y. Xiao and H. T. Soh, *Angew. Chem., Int. Edit.*, 2010, **49**, 355-358; (c) J. F. Rusling, *Anal. Chem.*, 2013, **85**, 5304-5310.
2. (a) N. L. Anderson and N. G. Anderson, *Mol. Cell. Proteomics*, 2002, **1**, 845-867; (b) R. Etzioni, N. Urban, S. Ramsey, M. McIntosh, S. Schwartz, B. Reid, J. Radich, G. Anderson and L. Hartwell, *Nat. Rev. Cancer*, 2003, **3**, 243-252; (c) L. Thadikkaran, M. A. Siegenthaler, D. Crettaz, P. A. Queloz, P. Schneider and J. D. Tissot, *Proteomics*, 2005, **5**, 3019-3034; (d) B. Pesch, T. Bruning, G. Johnen, S. Casjens, N. Bonberg, D. Taeger, A. Muller, D. G. Weber and T. Behrens, *Biochim. Biophys. Acta*, 2013, DOI: 10.1016/j.bbapap.2013.12.007.
3. (a) Y. J. Zhao, X. W. Zhao, J. Hu, M. Xu, W. J. Zhao, L. G. Sun, C. Zhu, H. Xu and Z. Z. Gu, *Adv. Mater.*, 2009, **21**, 569-572; (b) Y. J. Zhao, X. W. Zhao, J. Hu, J. Li, W. Y. Xu and Z. Z. Gu, *Angew. Chem., Int. Edit.*, 2009, **48**, 7350-7352; (c) G. Z. Deng, K. Xu, Y. Sun, Y. Chen, T. S. Zheng and J. L. Li, *Anal. Chem.*, 2013, **85**, 2833-2840.
4. (a) P. C. Lin, P. H. Chou, S. H. Chen, H. K. Liao, K. Y. Wang, Y. J. Chen and C. C. Lin, *Small*, 2006, **2**, 485-489; (b) K. Y. Wang, S. A. Chuang, P. C. Lin, L. S. Huang, S. H. Chen, S. Ouarda, W. H. Pan, P. Y. Lee, C. C. Lin and Y. J. Chen, *Anal. Chem.*, 2008, **80**, 6159-6167; (c) P. C. Lin, S. H. Chen, K. Y. Wang, M. L. Chen, A. K. Adak, J. R. R. Hwu, Y. J. Chen and C. C. Lin, *Anal. Chem.*, 2009, **81**, 8774-8782; (d) E. Stern, A. Vacic, N. K. Rajan, J. M. Criscione, J. Park, B. R. Ilic, D. J. Mooney, M. A. Reed and T. M. Fahmy, *Nat. Nanotechnol.*, 2010, **5**, 138-142.
5. (a) Y. S. Lin, P. J. Tsai, M. F. Weng and Y. C. Chen, *Anal. Chem.*, 2005, **77**, 1753-1760; (b) P. H. Chou, S. H. Chen, H. K. Liao, P. C. Lin, G. R. Her, A. C. Y. Lai, J. H. Chen, C. C. Lin and Y. J. Chen, *Anal. Chem.*, 2005, **77**, 5990-5997; (c) L. Zhao, H. Q. Qin, Z. Y. Hu, Y. Zhang, R. A. Wu and H. F. Zou, *Chem. Sci.*, 2012, **3**, 2828-2838; (d) Y. R. Ma, X. L. Zhang, T. Zeng, D. Cao, Z. Zhou, W. H. Li, H. Y. Niu and Y. Q. Cai, *ACS Appl. Mater. Inter.*, 2013, **5**, 1024-1030.
6. (a) C. S. Raska, C. E. Parker, S. W. Sunnarborg, R. M. Pope, D. C. Lee, G. L. Glish and C. H. Borchers, *J. Am. Soc. Mass Spectr.*, 2003, **14**, 1076-1085; (b) E. N. Warren, P. J. Elms, C. E. Parker and C. H. Borchers, *Anal. Chem.*, 2004, **76**, 4082-4092; (c) J. Jiang, C. E. Parker, J. R. Fuller, T. H. Kawula and C. H. Borchers, *Anal. Chim. Acta*, 2007, **605**, 70-79; (d) Y. Li, J. S. Wu, D. W. Qi, X. Q. Xu, C. H. Deng, P. Y. Yang and X. M. Zhang, *Chem. Commun.*, 2008, DOI: Doi 10.1039/B716055k, 564-566; (e) Y. Liu, Y. Li, J. Y. Liu, C. H. Deng and X. M. Zhang, *J. Am. Soc. Mass Spectr.*, 2011, **22**, 2188-2198.
7. (a) J. P. Nolan and L. A. Sklar, *Trends Biotechnol.*, 2002, **20**, 9-12; (b) H. Y. Hsu, T. O. Joos and H. Koga, *Electrophoresis*, 2009, **30**, 4008-4019.
8. Y. Rosenberg-Hasson, L. Hansmann, M. Liedtke, I. Herschmann and H. T. Maecker, *Immunol. Res.*, 2014, DOI: 10.1007/s12026-014-8491-6.
9. C. D. Walkey, J. B. Olsen, H. B. Guo, A. Emili and W. C. W. Chan, *J. Am. Chem. Soc.*, 2012, **134**, 2139-2147.
10. (a) N. Tang, P. Tornatore and S. R. Weinberger, *Mass. Spectrom. Rev.*, 2004, **23**, 34-44; (b) T. B. Martins, B. M. Pasi, C. M. Litwin and H. R. Hill, *Clin. Diagn. Lab. Immun.*, 2004, **11**, 325-329; (c) S. Pang, J. Smith, D. Onley, J. Reeve, M. Walker and C. Foy, *J. Immunol. Methods*, 2005, **302**, 1-12; (d) T. Waterboer, P. Sehr and M. Pawlita, *J. Immunol. Methods*, 2006, **309**, 200-204.
11. (a) T. Bryan, X. L. Luo, L. Forsgren, L. A. Morozova-Roche and J. J. Davis, *Chem. Sci.*, 2012, **3**, 3468-3473; (b) T. Bryan, X. L. Luo, P. R. Bueno and J. J. Davis, *Biosens. Bioelectron.*, 2013, **39**, 94-98.
12. X. L. Luo, M. Y. Xu, C. Freeman, T. James and J. J. Davis, *Anal. Chem.*, 2013, **85**, 4129-4134.
13. C. S. Jeon, I. Hwang and T. D. Chung, *Adv. Funct. Mater.*, 2013, **23**, 1484-1489.
14. (a) A. Chiu, W. K. Chan, S. H. Cheng, C. K. Leung and C. H. Choi, *Qjm-Mon. J. Assoc. Phys.*, 1999, **92**, 711-718; (b) M. I. Mohammed and M. P. Y. Desmulliez, *Lab. Chip*, 2011, **11**, 569-595.
15. J. V. Staros, R. W. Wright and D. M. Swingle, *Anal. Biochem.*, 1986, **156**, 220-222.
16. (a) H. Neubert, E. S. Jacoby, S. S. Bansal, R. K. Iles, D. A. Cowan and A. T. Kicman, *Anal. Chem.*, 2002, **74**, 3677-3683; (b) P. Peluso, D. S. Wilson, D. Do, H. Tran, M. Venkatasubbaiah, D. Quincy, B. Heidecker, K. Poindexter, N. Tolani, M. Phelan, K. Witte, L. S. Jung, P. Wagner and S. Nock, *Anal. Biochem.*, 2003, **312**, 113-124; (c) A. Kausaite-Minkstimiene, A. Ramanaviciene, J. Kirlyte and A. Ramanavicius, *Anal. Chem.*, 2010, **82**, 6401-6408.
17. J. Su and M. Mrksich, *Angew. Chem., Int. Edit.*, 2002, **41**, 4715-4718.
18. J. C. Love, L. A. Estroff, J. K. Kriebel, R. G. Nuzzo and G. M. Whitesides, *Chem. Rev.*, 2005, **105**, 1103-1169.
19. S. R. Sheth and D. Leckband, *Proc. Natl. Acad. Sci. U.S.A.*, 1997, **94**, 8399-8404.
20. A. Hennig, A. Hoffmann, H. Borcherding, T. Thiele, U. Schedler and U. Resch-Genger, *Anal. Chem.*, 2011, **83**, 4970-4974.
21. (a) L. H. Dubois and R. G. Nuzzo, *Annu. Rev. Phys. Chem.*, 1992, **43**, 437-463; (b) P. Li, J. J. Xu, Q. Wang and C. Wu, *Langmuir*, 2000, **16**, 4141-4147.
22. H. Hinterwirth, S. Kappel, T. Waitz, T. Prohaska, W. Lindner and M. Lammerhofer, *ACS Nano*, 2013, **7**, 1129-1136.
23. R. E. Ducker, S. Janusz, S. Q. Sun and G. J. Leggett, *J. Am. Chem. Soc.*, 2007, **129**, 14842-14843.

